ELSEVIER

Inorganica Chimica Acta 228 (1995) 199–206

Inorganica Chimica Acta

Structural, spectroscopic and redox characterization of the soluble complexes $[M(SC_6H_4NR_2)_4]^{2-}$ and the effects of N–H···S hydrogen bonds

Jiong Huang, John C. Dewan, M. Anton Walters *

Department of Chemistry, New York University, New York, NY 10003, USA

Received 14 April 1994; revised 13 June 1994

Abstract

The complex $[(C_2H_5)_4N]Na[Fe(SC_6H_4NH_2\text{-}2)_4]$ (**1**) has been synthesized in order to study the influence of ligand hydrogen bonding on the redox potential of monomeric iron–sulfur complexes. Compound **1** crystallizes in space group $P2_1/c$, with $a = 11.747(4)$, $b = 25.058(5)$, $c = 12.301(3)$ Å, $\beta = 106.22(2)°$ and $Z = 4$. The related cobalt complex $[(C_2H_5)_4N]_2[Co(SC_6H_4NH_2\text{-}2)_4]$ (**2**) was also synthesized and found to crystallize in space group *Pccn* with $a = 12.544(3)$, $b = 13.920(3)$, $c = 24.646(15)$ Å and $Z = 4$. The average M–S bond length is 2.341(1) Å in **1** and 2.295(2) Å in **2**. The electronic absorption spectrum of **2** is consistent with an equilibrium between the respective tetrahedral and pseudo-octahedral complexes $[Co(SC_6H_4NH_2\text{-}2)_4]^{2-}$ and $[Co(SC_6H_4NH_2\text{-}2)_3]^-$. The proton NMR spectra of **1** and **2** in saturated CD_3CN solutions show unusually broad, isotropically shifted ligand proton signals, indicative of exchange broadening. This result is consistent with the occurrence of $[M(SC_6H_4NH_2\text{-}2)_4]^{2-}$ complex anions in equilibrium with species that could not be identified by ^1H NMR. The cyclic voltammetry data for **1**, 12.0 mM in CH_3CN, show two irreversible redox waves with E_{ox} at −0.50 and −0.25 V, respectively, relative to SCE. The peak at −0.50 V is a likely candidate for the redox couple of the complex $[Fe(SC_6H_4NH_2\text{-}2)_4]^{2-}$. The peak at −0.25 V probably belongs to a pseudo-octahedral iron complex.

Keywords: Crystal structures; Electrochemistry; Iron complexes; Cobalt complexes; Thiolate complexes

1. Introduction

It has long been observed that the redox potentials of iron–sulfur proteins are significantly more positive than those of their synthetic models, when the latter are studied in environments of low polarity [1–6]. These differences in redox potential have been ascribed either to a high polarity in the region surrounding the protein metal center, or to hydrogen bonding interactions between the amide group of the peptide backbone and sulfur [2,7–10]. There have been many attempts to model the effects of hydrogen bonds on Fe–S protein redox potentials. In one series of studies, ligands of the type L = cys–X–Y–cys and cys–X–Y (where, for example, X–Y = pro–leu, gly–ala) were employed in the syntheses of the complexes represented by the formulas FeL_2, $Fe_2S_2L_2$ and $Fe_4S_4L_4$ [2,5,11–13]. These complexes have redox potentials that are close to those of Fe–S protein redox centers [14–17].

The positive shifts in the redox potentials of peptide–Fe complexes have been attributed to the effects of intraligand N–H···S hydrogen bonds [2,5,11–13]. In most studies the number and geometry of hydrogen bonds in such model compounds have not been well determined. Some recent reports on *o*-pivaloylaminobenzenethiolato, $[o\text{-}SC_6H_4NCOBu^t]^-$, complexes of iron(II) and cobalt(II) represent an attempt to ameliorate this situation [18]. However, because of the relative paucity of hydrogen-bonded model compounds, the redox effects of N–H···S hydrogen bonds remain poorly understood. Research in this laboratory has been designed to address this problem through the study of complexes in which both the structural and redox effects of N–H···S hydrogen bonds can be determined quantitatively. We report here on the synthesis, spectroscopic and electrochemical characterization of monomeric Fe and Co thiolate complexes and the effects of N–H···S hydrogen bonds in the solid and solution states.

* Corresponding author.

SSDI 0020-1693(94)04178-X

2. Experimental

All synthetic procedures were carried out under a nitrogen atmosphere either using Schlenk line techniques or in an inert-atmosphere glove box. Methanol, acetonitrile and ether were distilled and stored under nitrogen before use. All other reagents were purchased and used as received.

2.1. Synthesis of $[(C_2H_5)_4N]Na[Fe(SC_6H_4NH_2\text{-}2)_4]$ (1)

Ortho-aminobenzenethiol (5.01 g, 40.0 mmol) and sodium (0.92 g, 40.0 mmol) were allowed to react in methanol (30 ml) to generate $NaSC_6H_4NH_2$-2. The solution was stirred for 1 h, then evaporated under vacuum, leaving a white solid. The product was washed with THF and vacuum-dried (yield 4.63 g, 78%). $NaSC_6H_4NH_2$-2 (1.12 g, 7.62 mmol), $(C_2H_5)_4NBr$ (0.80 g, 3.81 mmol) and $FeBr_2$ (0.41 g, 1.91 mmol) were combined in methanol (30 ml) to give a yellow-green solution, which was stirred for 3 h and evaporated to dryness under vacuum, with gentle heating on a water bath. The solid thus obtained was dissolved in CH_3CN (30 ml), and the solution was filtered to remove NaBr. The solvent was removed under vacuum and the product was washed twice with ether, leaving a green solid (yield 1.10 g, 71%). Crystals suitable for X-ray crystallography were obtained by diffusion of ether vapor into a saturated CH_3CN solution of **1** containing one equivalent excess of ligand in the form $[(C_2H_5)_4N][SC_6H_4NH_2\text{-}2]$. The results were consistent with the presence of one equivalent each of acetonitrile and ethyl ether solvates. *Anal.* Found: C, 55.69; H, 6.82; N, 10.11. Calc. for $C_{38}H_{57}FeN_6NaS_4$: C, 55.59; H, 6.99; N, 10.24%.

2.2. Synthesis of $[(C_2H_5)_4N]_2[Co(SC_6H_4NH_2\text{-}2)_4]$ (2)

Sodium 2-aminobenzenethiolate, $NaSC_6H_4NH_2$-2 (1.07 g, 7.25 mmol), was combined with $(C_2H_5)_4NCl$ (0.60 g, 3.63 mmol) and $CoCl_2$ (0.24 g, 1.81 mmol) in methanol (40 ml). The resulting brown solution was stirred for 3 h, followed by solvent evaporation under vacuum with gentle heating. The resulting solid was dissolved in CH_3CN (40 ml), followed by filtration, then concentration under vacuum to a volume of 10 ml. The addition of ether (50 ml) afforded green crystals (yield 1.20 g, 81%). For X-ray crystallography, **2** was crystallized, as above, from CH_3CN/ether in the presence of one equivalent of excess ligand. *Anal.* Found: C, 58.73; H, 7.70; N, 10.20. Calc. for $C_{40}H_{64}N_6S_4Co$: C, 58.87; H, 7.90; N, 10.30%.

2.3. Synthesis of $HSC_6H_4N(CH_3)_2$-4

Dimethylaminothiophenol was synthesized according to literature methods [19,20]. Lithium (0.16 g, 0.11 mol) was added to a solution of 4-bromo-*N*,*N*-dimethylaniline (10.0 g, 0.050 mol) in ether (30 ml). The solution was refluxed for 3.5 h and stirred at room temperature overnight. Propylene sulfide (3.9 ml, 0.05 mol) was added slowly to the filtrate with the evolution of heat and the formation of a white precipitate. The solution was stirred overnight and filtered. The filter pad was washed with ether and the filtrates were combined, poured into ice water (80 ml), and stirred until all the solids dissolved. The ether layer was washed with 10% NaOH (aq) and the aqueous layers were combined and neutralized with HCl. The product, 4-dimethylaminothiophenol, was extracted with 200 ml of ether and dried over Na_2SO_4. The product was purified by distillation and obtained as a white crystalline solid on cooling to room temperature (yield 1.9 g, 25%). The ^1H NMR spectrum of 4-dimethylaminothiophenol in Me_2SO-d_6 showed resonances at 7.04, 6.52 ($-C_6H_4$), 4.66 (–SH) and 2.73 ($-N(CH_3)_2$) ppm.

2.4. Synthesis of $[(C_2H_5)_4N]_2[Fe\{SC_6H_4N(CH_3)_2\text{-}4\}_4]$ (3)

4-Dimethylaminothiophenol (1.67 g, 0.01 mol) and Na (0.25 g, 0.01 mol) were combined in methanol (30 ml), and gave the sodium thiolate salt as a white solid after evaporation of the solvent. $Na[SC_6H_4N(CH_3)_2\text{-}4]$ (0.75 g, 4.3 mmol), $FeCl_2$ (0.12 g, 0.97 mmol) and Et_4NCl (0.32 g, 1.9 mmol) were combined in methanol (25 ml) and stirred overnight. The solvent was evaporated with gentle heating under vacuum. The product was washed with ether and dried under vacuum, leaving a green powder (yield 0.55 g, 61%). Product identification was established by ^1H NMR (Section 3.2.3), which also revealed the presence of one equivalent of excess ligand $[SC_6H_4N(CH_3)_2\text{-}4]^-$ and counter-ion Et_4N^+. We were unable to remove this excess, and therefore relied on NMR to determine the nature of the product.

2.5. Instrumentation

Elemental analyses were carried out by Galbraith Laboratories. Proton NMR data were collected using a General Electric QE 300 (300 MHz) spectrometer. IR data were collected at a resolution of 4 cm^{-1} on a Nicolet 5DXB spectrometer using a solution cell with a 1.0 mm pathlength. Electronic absorption spectra were acquired on a Hewlett-Packard 8452A diode array spectrophotometer using HP 84530A MS DOS–UV/VIS operating software (version 1.0). The spectrometer

Table 1
Crystallographic data for $[(C_2H_5)_4N]Na[Fe(SC_6H_4NH_2\text{-}2)_4]$ (**1**) and $[(C_2H_5)_4N]_2[Co(SC_6H_4NH_2\text{-}2)_4]$ (**2**)

	1	**2**
Chemical formula	$C_{32}H_{44}NaFeN_5S_4$	$C_{40}H_{64}CoN_6S_4$
Formula weight	705.81	816.16
Space group	$P2_1/c$ (No. 14)	$Pccn$ (No. 56)
a (Å)	11.747(4)	12.544(3)
b (Å)	25.058(5)	13.920(3)
c (Å)	12.301(3)	24.646(15)
β (°)	106.22(2)	
V (Å^3)	3477(2)	4303(6)
Z	4	4
T (°C)	−100	25
λ (Å)	1.54178	1.54178
ρ_{calc} (g cm^{-3})	1.348	1.260
μ (cm^{-1})	60.56	53.20
Trans. coeff.	0.87–1.09	0.77–1.19
R_1	0.040	0.070
R_2	0.050	0.081

was controlled by a Zenith Data Systems ZDE-1217-A0 computer.

2.6. X-ray crystallography

X-ray data (Tables 1, 2 and 3) were collected on a Rigaku AFC-6R diffractometer employing Cu Kα radiation. For **1** the sample was mounted on a glass fiber and cooled under a flow of nitrogen gas. A total of 5523 reflections were collected at −100 °C in the range $4.0° < 2\theta < 119.3°$. Of these, 4229 reflections with $I_o > 2\sigma(I_o)$ were used in the structure refinement, which was carried out by full-matrix least-squares techniques (389 variables) with the TEXSAN crystallographic software package. Hydrogen atoms were placed in calculated positions except for those of the $-NH_2$ groups, which could not be located and were ignored. All nonhydrogen atoms were refined anisotropically. The final difference-Fourier map showed no chemically significant features.

A single crystal of complex **2** was mounted on a glass fiber and coated in epoxy for data acquisition. A total of 3072 reflections were collected at 25 °C in the range $4.0° < 2\theta < 109.9°$ on the AFC-6R diffractometer. Of these, the 1923 reflections with $I_o > 2\sigma(I_o)$ were used in the structure refinement (268 variables). The cations of this structure suffer some disorder, and their hydrogen atoms were ignored, while those of the anion were placed in calculated positions. All nonhydrogen atoms were refined anisotropically. The final difference-Fourier map showed no chemically significant features.

3. Results and discussion

The *ortho*-aminothiolate ion, $[SC_6H_4NH_2\text{-}2]^-$, has the capacity to act as a bidentate ligand. It has been reported to form neutral four-coordinate complexes, $M(SC_6H_4NH_2\text{-}2)_2$, with divalent metal ions [21]. A ligand-to-metal ratio of 4:1 in CH_3CN solution, however, gave crystallization products having four-coordinate monodentate sulfur ligation of Fe(II), **1**, and Co(II), **2**. In solution, these complexes show evidence of partial ligand dissociation accompanied by rearrangement of the resulting complexes.

Table 2
The final atomic coordinates for nonhydrogen atoms in $[(C_2H_5)_4N]Na[Fe(SC_6H_4NH_2\text{-}2)_4]$ (**1**)

Atom	x	y	z
Fe	0.27221(5)	0.32043(2)	0.97564(5)
Na	0.3307(1)	0.23709(6)	0.7519(1)
S(1)	0.34750(8)	0.35183(4)	0.83131(8)
S(2)	0.26000(9)	0.37447(4)	1.12679(8)
S(3)	0.37172(8)	0.23951(4)	1.03078(8)
S(4)	0.07160(8)	0.29555(4)	0.93313(8)
N(11)	0.2399(3)	0.3736(1)	0.5760(3)
N(21)	0.2943(4)	0.4211(2)	1.3555(3)
N(31)	0.5010(3)	0.1889(1)	0.8793(3)
N(41)	0.1154(3)	0.2512(1)	0.7146(3)
C(11)	0.2505(3)	0.4049(1)	0.7684(3)
C(12)	0.2056(3)	0.4094(2)	0.6502(3)
C(13)	0.1292(4)	0.4510(2)	0.6046(3)
C(14)	0.0962(4)	0.4876(2)	0.6731(4)
C(15)	0.1399(4)	0.4841(2)	0.7881(4)
C(16)	0.2165(4)	0.4428(2)	0.8353(3)
C(21)	0.3913(4)	0.4062(1)	1.2064(3)
C(22)	0.3940(4)	0.4250(2)	1.3159(3)
C(23)	0.4985(5)	0.4489(2)	1.3806(4)
C(24)	0.5957(5)	0.4545(2)	1.3419(5)
C(25)	0.5940(5)	0.4357(2)	1.2348(5)
C(26)	0.4904(4)	0.4124(2)	1.1679(4)
C(31)	0.5233(3)	0.2512(1)	1.0376(3)
C(32)	0.5726(3)	0.2245(2)	0.9609(3)
C(33)	0.6904(4)	0.2340(2)	0.9657(3)
C(34)	0.7595(4)	0.2688(2)	1.0447(4)
C(35)	0.7109(4)	0.2938(2)	1.1205(4)
C(36)	0.5942(4)	0.2852(2)	1.1164(4)
C(41)	0.0365(3)	0.2308(1)	0.8747(3)
C(42)	0.0574(3)	0.2160(2)	0.7720(3)
C(43)	0.0234(3)	0.1656(2)	0.7265(3)
C(44)	−0.0321(4)	0.1299(2)	0.7807(3)
C(45)	−0.0538(4)	0.1441(2)	0.8818(3)
C(46)	−0.0190(3)	0.1939(2)	0.9275(3)

3.1. Crystal structures

In compound **1** a sodium cation and a $[(C_2H_5)_4N]^+$ ion serve to balance the −2 charge of the complex anion. The anion has C_1 symmetry, with N(31), N(41), S(1), S(2) and S(3) coordinated to Na cations (Fig. 1, Table 4). In **2**, where both counter-ions are $[(C_2H_5)_4N]^+$, the anion has approximate S_4 symmetry (Fig. 2). The average M–S bond lengths are 2.341(1) Å in **1** and 2.295(2) Å in **2** (Table 4). These values are similar to the average M–S bond lengths of 2.353(9) and 2.328(11) Å in the non-hydrogen-bonding complexes $[(C_6H_5)_4$-

Table 3
The final atomic coordinates for the nonhydrogen atoms in $[(C_2H_5)_4N]_2[Co(SC_6H_4NH_2\text{-}2)_4]$ (2)

Atom	x	y	z
Co	0.2500	0.7500	0.31540(5)
S(1)	0.3603(2)	0.6502(1)	0.26837(8)
S(2)	0.1408(2)	0.6484(1)	0.36446(7)
N(11)	0.5132(6)	0.5516(5)	0.1968(3)
N(21)	0.0400(6)	0.5099(6)	0.4402(3)
N(31)	0.7500	0.2500	0.4366(3)
N(41)	0.2500	0.2500	0.1740(3)
C(11)	0.4471(6)	0.7097(6)	0.2236(3)
C(12)	0.4512(6)	0.8068(6)	0.2178(3)
C(13)	0.5215(7)	0.8527(7)	0.1824(3)
C(14)	0.5884(8)	0.794(1)	0.1515(3)
C(15)	0.5849(7)	0.6960(8)	0.1563(4)
C(16)	0.5149(6)	0.6521(7)	0.1918(3)
C(21)	0.2105(6)	0.5692(5)	0.4070(3)
C(22)	0.3199(7)	0.5645(6)	0.4097(3)
C(23)	0.3740(7)	0.5023(7)	0.4438(3)
C(24)	0.315(1)	0.4420(7)	0.4765(4)
C(25)	0.207(1)	0.4443(7)	0.4747(4)
C(26)	0.1518(8)	0.5068(6)	0.4407(3)
C(31A)	0.746(2)	0.362(1)	0.4353(7)
C(31B)	0.766(4)	0.292(1)	0.3829(6)
C(32)	0.763(1)	0.4091(6)	0.3851(4)
C(33A)	0.873(1)	0.234(2)	0.4379(8)
C(33B)	0.782(6)	0.289(2)	0.4899(7)
C(34)	0.9330(8)	0.250(1)	0.4876(5)
C(41A)	0.127(1)	0.250(2)	0.1614(7)
C(41B)	0.201(2)	0.309(2)	0.1229(8)
C(42)	0.093(1)	0.321(1)	0.1217(6)
C(43A)	0.196(2)	0.155(1)	0.177(1)
C(43B)	0.264(2)	0.195(1)	0.2295(6)
C(44)	0.247(1)	0.0887(6)	0.2250(4)

P]$_2$[M$(SC_6H_5)_4$] (M = Fe, Co) [22,23]. They are nearly identical to the corresponding metal–ligand bond lengths (2.329 and 2.296 Å) of the N–H···S hydrogen-bonded complexes $[(C_2H_5)_4N]_2[M(o\text{-}SC_6H_4NCOBu^t)_4]$, where M = Fe and Co, respectively [18]. The *ortho* substituents of the ligand phenyl rings, sulfur and $-NH_2$, are separated by 2.968(4)–3.089(3) Å in **1**, and 2.945(7)–2.966(7) Å in **2** (Table 4). There is evidence of intermolecular hydrogen bonding in both **1** and **2**, with N···S distances in the range 3.35–3.55 Å (Table 4).

The complex anions $[M(SC_6H_5)_4]^{2-}$ are known to occur in either of two high-symmetry forms, S_4 and D_{2d} [22–24]. Just as is observed in compound **2**, S_4 symmetry has previously been reported for complexes with $[R_4N]^+$ counter-ions [22,25–27]. In S_4 symmetry, bonding between the S atom lone-pair p orbital and the π orbitals of the phenyl ring is disrupted [22]. This disruption is due to intraligand N–H···S hydrogen bonding, which tends to involve the sulfur p orbital perpendicular to the C–S–Fe plane [28]. In complex **1** the lowering of symmetry to C_1 results from the coordination of Na^+ by the anion.

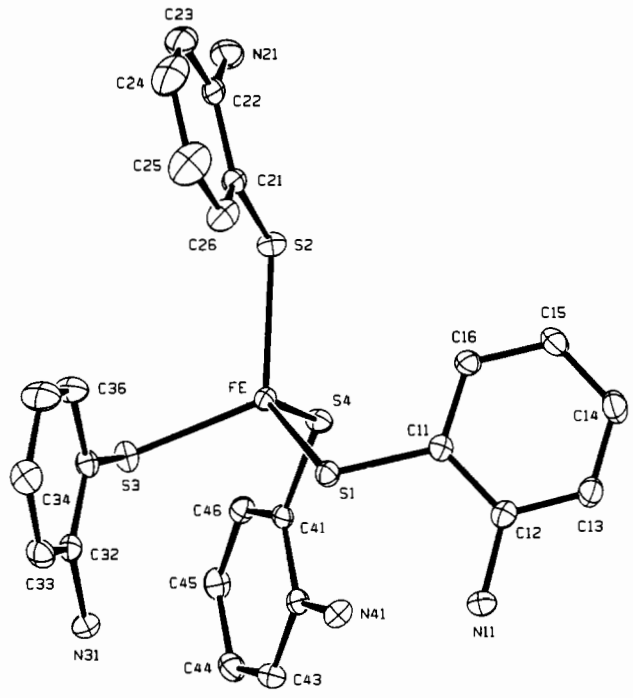

Fig. 1. ORTEP diagram of the complex anion $[Fe(SC_6H_4NH_2\text{-}2)_4]^{2-}$ in **1** showing the atom labeling scheme and 30% probability thermal ellipsoids.

Table 4
Selected bond lengths and angles for $[(C_2H_5)_4N]Na[Fe(SC_6H_4NH_2\text{-}2)_4]$ (**1**) and $[(C_2H_5)_4N]_2[Co(SC_6H_4NH_2\text{-}2)_4]$ (**2**)

1		2	
Fe–S(1)	2.330(1)	Co–S(1)	2.278(2)
Fe–S(2)	2.337(1)	Co–S(2)	2.278(2)
Fe–S(3)	2.344(1)	Co–S(3)	2.311(2)
Fe–S(4)	2.351(1)	Co–S(4)	2.311(2)
Na–N(31)	2.483(4)		
Na–N(41)	2.466(4)		
Na–S(1)	3.025(2)		
Na–S(3)	3.329(2)		
Na–S(2) [a]	3.187(2)		
Na–S(3) [a]	2.950(2)		
S(1)···N(11)	3.089(3)	S(1)···N(11)	2.945(7)
S(2)···N(21)	2.968(4)	S(2)···N(21)	2.966(7)
S(3)···N(31)	2.994(3)		
S(4)···N(41)	3.083(3)		
S(3)···N(11) [b]	3.349(4)	S(2)···N(11) [c]	3.548(7)
S(4)···N(41) [b]	3.553(3)		
S(1)–Fe–S(2)	122.09(4)	S(1)–Co–S(1)	118.8(1)
S(1)–Fe–S(3)	104.35(4)	S(1)–Co–S(2)	104.66(7)
S(1)–Fe–S(4)	119.35(4)	S(1)–Co–S(2)	106.22(7)
S(2)–Fe–S(3)	114.05(4)	S(1)–Co–S(2)	106.22(7)
S(2)–Fe–S(4)	92.88(4)	S(1)–Co–S(2)	104.66(7)
S(3)–Fe–S(4)	102.88(4)	S(2)–Co–S(2)	116.9(1)

[a] The sulfur atom is at position $(x, \frac{1}{2}-y, -\frac{1}{2}+z)$.

[b] The nitrogen atom is at position $(x, \frac{1}{2}-y, -\frac{1}{2}+z)$, intermolecular hydrogen bond.

[c] The nitrogen atom is at position $(-\frac{1}{2}+x, 1+y, \frac{1}{2}+z)$, intermolecular hydrogen bond.

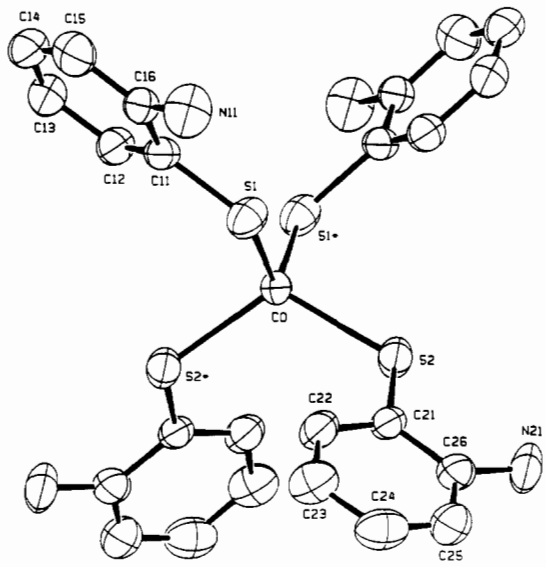

Fig. 2. ORTEP diagram of the complex anion $[Co(SC_6H_4NH_2\text{-}2)_4]^{2-}$ in **2** showing the atom labeling scheme and 30% probability thermal ellipsoids. The Co atom lies on a twofold axis. Atoms marked with an asterisk are related to unmarked atoms by an axis of rotation.

3.2. Spectroscopic measurements

3.2.1. Infrared spectroscopy

Hydrogen bonding in the *ortho*-aminobenzenethiolate ligand is maintained by the proximity of the sulfur and amine ring substituents. In the absence of hydrogen bonding, the frequency difference between the symmetric and asymmetric $-NH_2$ stretching modes can be predicted by the empirical equation [29–32]

$$\Delta\nu = \nu_{as} - \nu_s = 0.4219\nu_s - 1348.2\ cm^{-1} \quad (1)$$

where ν_s and ν_{as} denote symmetric and asymmetric stretching mode frequencies, respectively. In hydrogen-bonded arylaminothiols, ν_{as} undergoes a positive deviation relative to the frequency predicted using Eq. (1). The magnitude of the deviation is proportional to the strength of the hydrogen bond [32,33]. In saturated CH_3CN solution, two bands corresponding to $\nu_{as}(NH_2)$ and $\nu_s(NH_2)$ for $HSC_6H_4NH_2$-2 occur at 3463 and 3372 cm^{-1}, respectively, as compared with $[SC_6H_4NH_2\text{-}2]^-$, which has peaks at 3429 and 3280 cm^{-1}. The corresponding frequency shifts are $\Delta\nu_{pred}=74$, $\Delta\nu_{obs}=91$ cm^{-1} for $HSC_6H_4NH_2$-2 and $\Delta\nu_{pred}=36$, $\Delta\nu_{obs}=150$ cm^{-1} for $[SC_6H_4NH_2\text{-}2]^-$. Evidently, N–H···S hydrogen bonding exists in both forms of the *ortho*-aminothiol ligand, although it is greatly enhanced in the deprotonated state. On this basis it is expected that hydrogen bonding persists in complexes **1** and **2**, where much of the electron density of the dianion resides on sulfur [34]. The determination of $\Delta\nu$ for complexes **1** and **2** is complicated by an equilibrium mixture of species in solution, which is discussed below.

3.2.2. Electronic absorption spectroscopy

The electronic absorption spectrum of **2** reveals bands at 566, 636, 700 and 736 nm in CH_3CN solution. Except for the band at 566 nm, the spectrum of **2** corresponds closely to that of the tetrahedral complex anion $[Co(SC_6H_5)_4]^{2-}$, which has bands at 625, 680 and 725 nm [23,35,36]. The band at 566 nm in **2** is noteworthy because it corresponds to d–d transitions of an octahedral or pseudo-octahedral Co(II) complex anion [37]. The intensity of this band increases with time, signaling an increase in the concentration of pseudo-octahedrally coordinated Co(II). While the band at 566 nm is small relative to the absorption band manifold of the tetrahedral complex, its extinction coefficient is expected to be approximately 100 times smaller than that of the latter [38] and therefore indicates a significant concentration of pseudo-octahedral complex. Complex **2** probably undergoes ligand displacement and rearrangement in accordance with the scheme

$$[Co(SC_6H_4NH_2\text{-}2)_4]^{2-} = [Co(SC_6H_4NH_2\text{-}2)_3]^- + [SC_6H_4NH_2\text{-}2]^- \quad (2)$$

In the solid state (KBr pellet), **2** has electronic absorption bands at 572, 660, 700 and 740 nm. The 660–740 nm bands correspond to those of $[Co(SC_6H_5)_4]^{2-}$. The band at 572 nm is unexpected and may correspond to a structural rearrangement product, $[Co(SC_6H_4NH_2\text{-}2)_3]^-$, generated by trituration in the preparation of the pellet.

3.2.3. Nuclear magnetic resonance

Complexes **1–3** are paramagnetic and exhibit ^1H NMR spectra (Fig. 3) characteristic of the four-coordinate benzenethiolato complexes $[M(SC_6H_5)_4]^{2-}$, where M = Fe, Co [39,40]. Assignments for **1** in saturated (12.0 mM) CD_3CN are −19.6 (*o,p*-H), 21.9 (*m*-H) and 27.9 ($-NH_2$) ppm. These resonances, which change little

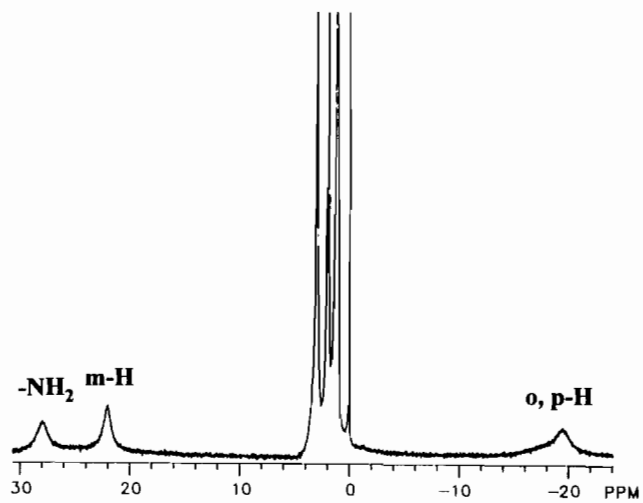

Fig. 3. Proton NMR spectrum of **1** recorded in CD_3CN at room temperature.

Table 5
Redox potentials (V) for selected iron benzenethiolate complexes [a]

Compound	$E_{ox}(1)$	$E_{ox}(2)$
$[(C_2H_5)_4N]Na[Fe(SC_6H_4NH_2\text{-}2)_4]$ (1), 12.0 mM	−0.50	−0.25
$[(C_2H_5)_4N]Na[Fe(SC_6H_4NH_2\text{-}2)_4]$ (1), 5.0 mM	−0.48	−0.26
$[(C_2H_5)_4N]_2[Fe(SC_6H_4N(CH_3)_2\text{-}4)_4]$ (3), 10.0 mM	−0.72	
$[(C_2H_5)_4N]_2[Fe(SC_6H_5)_4]$	−0.51	

[a] Solvent CH_3CN, electrolyte $[(C_2H_5)_4N]ClO_4$, 0.1 M. Scan rate 200 mV s^{-1}, ambient temperature, glassy carbon working electrode, calomel reference electrode, and Pt wire counter electrode.

over the temperature range 25 to −20 °C, are broad relative to those of $[Fe(SC_6H_5)_4]^{2-}$, for which the room-temperature assignments are −23.5 (*p*-H), −16.8 (*o*-H) and 22.3 (*m*-H) ppm [39]. The proton resonances of **1** are probably exchange broadened owing to a fast structural rearrangement involving ligand exchange. The ^1H NMR spectrum of **2**, recorded at ambient temperature in a saturated CD_3CN solution, is featureless, probably owing to the same processes as in **1** but occurring at a faster rate. In support of this interpretation is the fact that at −20 °C a spectrum is observed for **2** which is quite similar to that of **1**. The ligand proton resonance assignments for **2** at low temperature are −32.2 (*o,p*-H), 16.8 (*m*-H) and 28.4 ($-NH_2$) ppm. This spectrum compares favorably with that of the anion $[Co(SC_6H_5)_4]^{2-}$, which has resonances at −34.0 (*o*-H), −26.6 (*p*-H) and 16.7 (*m*-H) ppm at room temperature [40]. The room-temperature ^1H NMR spectrum of **3** in saturated (10.0 mM) CD_3CN solution revealed relatively sharp resonances at −17.8 (*o*-H), 7.72 ($-N(CH_3)_2$) and 21.6 (*m*-H) ppm.

Whereas complexes **1** and **2** exhibit features characteristic of rapid ligand exchange, complex **3** does not, as evidenced by its relatively sharp proton resonance peaks. Presumably, ligand exchange in **1** and **2** is driven by linkage isomerization, which can occur with *ortho*-aminobenzenethiolate but not with *para*-dimethylaminobenzenethiolate.

3.2.4. Cyclic voltammetry

Redox potentials were measured for complexes **1** and **3** in CH_3CN (Table 5). For complex **1**, two irreversible redox waves are observed which exhibit concentration-dependent behavior. In a saturated (12.0 mM) CH_3CN solution the cyclic voltammogram of **1** is stable and has two irreversible redox waves showing oxidation peaks at −0.50 and −0.25 V relative to SCE. In a 5.0 mM solution, we observed oxidation peaks at −0.48 and −0.26 V (Fig. 4(a)); the more negative peak slowly disappears with time (Fig. 4(b)). If we assume that complexes **1** and **2** undergo similar structural rearrangements in solution, the decrease in the height of the −0.48 V peak may result from the disappearance of an Fe tetrahedral complex. Based on this interpretation, the −0.48 V oxidation peak probably corresponds

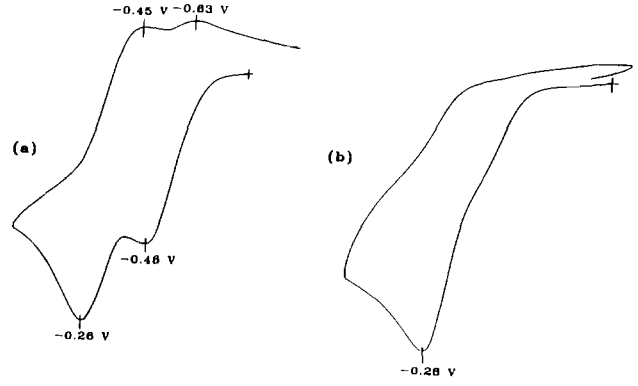

Fig. 4. Cyclic voltammograms of $[Fe(SC_6H_4NH_2\text{-}2)_4]^{2-}$ (5.0 mM) in CH_3CN at two time points: (a) $t=1$ min; (b) $t=40$ min. Data were recorded at room temperature at a scan rate of 200 mV s^{-1}, using a glassy carbon working electrode, Pt wire counter electrode, and calomel reference electrode. The solutions contained Et_4NClO_4 (0.10 M) as a supporting electrolyte.

to the Fe(II)/Fe(III) oxidation of **1**. The peak at −0.26 V, which does not correspond to the oxidation of a free ligand, may instead belong to the Fe(II)/Fe(III) redox couple of a pseudo-octahedral complex anion, $[Fe(SC_6H_4NH_2\text{-}2)_3]^-$.

Concentration-dependent effects such as those observed in the cyclic voltammograms of **1** are well known in metal thiolate chemistry. Dance [36] has pointed out that the equilibria between various complexes with the formula $\{Co(SC_6H_5)_4[Co(SC_6H_5)_2]_n\}^{2-}$, $n=0,3$, are sensitive to both solvent polarity and temperature. Costa et al. [41] observed concentration-dependent equilibria in the formation of the ethane dithiolate complex ion, $[Mn(S_2C_2H_4)_2]^{2-}$, in acetonitrile. In the light of these results, a concentration-dependent solvolysis of **1** is quite plausible.

The complex anion of **3**, $[Fe(SC_6H_4N(CH_3)_2\text{-}4)_4]^{1-/2-}$, exhibits an oxidation wave at −0.72 V in CH_3CN at a concentration of 10.0 mM. Because of the electron-donating characteristics of the *para*-dimethylamine substituent, its oxidation peak is 210 mV more negative than the oxidation peak of $[Fe(SC_6H_5)_4]^{2-}$, at −0.51 V [39]. A similar effect is observed in the comparison of the redox potentials of the ions $[Fe_4S_4(SC_6H_5)_4]^{2-/3-}$ and $[Fe_4S_4(SC_6H_5NH_2\text{-}4)_4]^{2-/3-}$, which have redox potentials of −1.04 and −1.14 V, respectively [2,42].

The *ortho*-amino group in **1** should likewise cause a decrease in the redox potential relative to that reported for the non-hydrogen-bonding complex anion $[Fe(SC_6H_5)_4]^{2-}$. However, the first oxidation peak of **1** is virtually identical to that of $[Fe(SC_6H_5)_4]^{2-}$. On the basis of comparisons with complex **3**, the redox potential of **1** may be at least 220 mV more positive than expected. Such a positive shift could be ascribed to the effects of N–H···S hydrogen bonds. Redox potential shifts of this magnitude have previously been attributed to the electron-withdrawing effects of hydrogen bonds to sulfur ligands in Fe–S proteins and their model complexes.

4. Conclusions

Although complexes **1** and **2** appear to undergo rearrangement, we have attempted to identify those spectroscopic and electrochemical features that belong, exclusively, to the tetrahedral complexes observed by X-ray crystallography. Our assignments suggest that the redox properties are affected both by N–H···S hydrogen bonding and by inductive effects through the ligand phenyl rings. A similar situation may hold for related compounds such as $[(C_2H_5)_4N]_2[M(o\text{-}SC_6H_4NCOBu^t)_4]$ [18]. Hydrogen bonding and through-bond inductive effects may be opposed in *ortho*-aminobenzenethiolate, thus masking the positive shift of the redox potential in $[Fe(SC_6H_4NH_2\text{-}2)_4]^{2-}$ (**1**) relative to that in $[Fe(SC_6H_5)_4]^{2-}$. However, by estimating the magnitude of the expected redox potential shift in the absence of electron donation from the $-NH_2$ group, it appears that the four N–H···S hydrogen bonds in **1** account for a shift of approximately +240 mV in the redox potential of **1** relative to $[Fe(SC_6H_5)_4]^{2-}$.

5. Supplementary material

General structure reports for **1** and **2**, including details of the structure determination, listings of experimental details, positional and thermal parameters, inter- and intramolecular bond distances and bond angles involving nonhydrogen atoms, intermolecular distances involving hydrogen atoms, PLUTO diagrams of the structures, and a listing of final observed and calculated structure factors, are available from the authors.

Acknowledgements

We wish to thank Professor David Gosser for helpful discussions, and Professor Andrew Bocarsly and Mr Longchun Cheng for assistance in the acquisition and interpretation of electrochemical data. This investigation has been supported by the Exxon Education Foundation and by the National Science Foundation (Grant No. CHE-9203455 to M.A.W.).

References

[1] R.W. Lane, J.A. Ibers, R.B. Frankel and R.H. Holm, *Proc. Natl. Acad. Sci. USA, 72* (1975) 2868.
[2] B.V. DePamphilis, B.A. Averill, T. Herskovitz, L. Que, Jr., and R.H. Holm, *J. Am. Chem. Soc., 96* (1974) 4159.
[3] L. Que, Jr., J.R. Anglin, M.A. Bobrik, A. Davison and R.H. Holm, *J. Am. Chem. Soc., 96* (1974) 6042.
[4] J.J. Mayerle, S.E. Denmark, B.V. DePamphilis, J.A. Ibers and R.H. Holm, *J. Am. Chem. Soc., 97* (1975) 1032.
[5] C.L. Hill, J. Renaud, R.H. Holm and L.E. Mortenson, *J. Am. Chem. Soc., 99* (1977) 2549.
[6] R.W. Lane, J.A. Ibers, R.B. Frankel, G.C. Papaefthymiou and R.H. Holm, *J. Am. Chem. Soc., 99* (1977) 84.
[7] G. Backes, Y. Mino, T.M. Loehr, T.E. Meyer, M.A. Cusanovich, W.V. Sweeney, E.T. Adman and J. Sanders-Loehr, *J. Am. Chem. Soc., 113* (1991) 2055.
[8] C.W.J. Carter, *J. Biol. Chem., 252* (1977) 7802.
[9] R. Ohno, N. Ueyama and A. Nakamura, *Inorg. Chem., 30* (1991) 4887.
[10] W.W. Smith, R.M. Burnett, G.D. Darling and M.L. Ludwig, *J. Mol. Biol., 117* (1977) 195.
[11] N. Ueyama, M. Nakata, M.-A. Fuji, T. Terakawa and A. Nakamura, *Inorg. Chem., 24* (1985) 2190.
[12] M. Nakata, N. Ueyama, M.-A. Fuji, A. Nakamura, K. Wada and H. Matsubara, *Biochim. Biophys. Acta, 788* (1984) 306.
[13] A. Nakamura and N. Ueyama, in L. Que (ed.), *Metal Clusters in Proteins*, American Chemical Society, Washington, DC, 1988, Ch. 14.
[14] W. Lovenberg and B.E. Sobel, *Proc. Natl. Acad. Sci. USA, 54* (1965) 193.
[15] D.J. Newman and J.R. Postgate, *Eur. J. Biochem., 7* (1968) 45.
[16] J.A. Peterson and M.J. Coon, *J. Biol. Chem., 243* (1968) 339.
[17] I. Moura, J.J.G. Moura, M.H. Santos, A.V. Xavier and J. LeGall, *FEBS Lett., 107* (1979) 419.
[18] (a) N. Ueyama, T.-A. Okamura and A.J. Nakamura, *J. Chem. Soc., Chem. Commun.*, (1992) 1019; (b) A. Nakamura, N. Ueyama, T.-A. Okamura and S. Takamizawa, *J. Inorg. Biochem., 51* (1993) 30; (c) N. Ueyama, T.-A. Okamura and A. Nakamura, *J. Am. Chem. Soc., 114* (1992) 8129.
[19] H. Gilman, E.A. Zoellner and W.M. Selby, *J. Am. Chem. Soc., 55* (1933) 1252.
[20] F.G. Bordwell and P.J. Boutan, *J. Am. Chem. Soc., 78* (1956) 854.
[21] L.F. Larkworthy, J.M. Murphy and D.J. Phillips, *Inorg. Chem., 7* (1968) 1436.
[22] D. Coucouvanis, D. Swenson, N.C. Baenziger, C. Murphy, D.G. Holah, N. Sfarnas, A. Simopoulos and A. Kostikas, *J. Am. Chem. Soc., 103* (1981) 3350.
[23] D. Swenson, N.C. Baenziger and D. Coucouvanis, *J. Am. Chem. Soc., 100* (1978) 1932.
[24] K. Fukui, H. Ohya-Nishiguchi and N. Hirota, *Bull. Chem. Soc. Jpn., 64* (1991) 1205.
[25] N. Ueyama, T. Sugawara, K. Sasaki, A. Nakamura, S. Yamashita, Y. Wakatsuki, H. Yamazaki and N. Yasuoka, *Inorg. Chem., 27* (1988) 741.
[26] T. Yamamura, H. Miyamae, Y. Katayama and Y. Sasaki, *Chem. Lett.*, (1985) 269.

[27] S.A. Koch, L.E. Maelia and M. Millar, *J. Am. Chem. Soc., 105* (1983) 5944.
[28] R.E. Rosenfield, Jr., R. Parthasarathy and J.D. Dunitz, *J. Am. Chem. Soc., 99* (1977) 4860.
[29] L.J. Bellamy and R.L. Williams, *Spectrochim. Acta, 9* (1957) 341.
[30] P.J. Krueger, *Can. J. Chem., 40* (1962) 2300.
[31] A.N. Hambly and B.V. O'Grady, *Aust. J. Chem., 15* (1962) 626.
[32] P.J. Krueger, *Tetrahedron, 26* (1970) 4753.
[33] H. Wolff and D.Z. Staschewski, *Z. Elektrochem., 66* (1962) 140.
[34] L. Noodleman, J.G. Norman, Jr., J.H. Osborne, A. Aizman and D. Case, *J. Am. Chem. Soc., 107* (1985) 3418.
[35] D.G. Holah and D. Coucouvanis, *J. Am. Chem. Soc., 97* (1975) 6918.
[36] I.G. Dance, *J. Am. Chem. Soc., 101* (1979) 6264.
[37] F.A. Cotton and G. Wilkinson, *Advanced Inorganic Chemistry*, Wiley, New York, 1988, p. 730, and references therein.
[38] B.N. Figgis, *Introduction to Ligand Fields*, Wiley, New York, 1966, Ch. 9.
[39] K.S. Hagen, J.G. Reynolds and R.H. Holm, *J. Am. Chem. Soc., 103* (1981) 4054.
[40] (a) M.A. Walters, J.C. Dewan, C. Min and S. Pinto, *Inorg. Chem., 30* (1991) 2656; (b) W.P. Chung, J.C. Dewan and M.A. Walters, *J. Am. Chem. Soc., 113* (1991) 525.
[41] T. Costa, J.R. Dorfman, K.S. Hagen and R.H. Holm, *Inorg. Chem., 22* (1983) 4091.
[42] T.J. Ollerenshaw, C.D. Garner, B. Odell and W.J. Clegg, *J. Chem. Soc., Dalton Trans.*, (1985) 2161.